Development 129, 1623-1632 (2002)
Printed in Great Britain © The Company of Biologists Limited 2002
DEV8909

The elongation factors Pandora/Spt6 and Foggy/Spt5 promote transcription in the zebrafish embryo

Brian R. Keegan[1,*], Jessica L. Feldman[1,*], Diana H. Lee[1], David S. Koos[2], Robert K. Ho[2], Didier Y. R. Stainier[3] and Deborah Yelon[1,†]

[1]Developmental Genetics Program and Department of Cell Biology, Skirball Institute of Biomolecular Medicine, New York University School of Medicine, New York, NY, USA
[2]Department of Molecular Biology, Princeton University, Princeton, NJ, USA
[3]Department of Biochemistry and Biophysics and Programs in Developmental Biology, Genetics, and Human Genetics, University of California, San Francisco, San Francisco, CA, USA
*These authors contributed equally to the work
[†]Author for correspondence (e-mail: yelon@saturn.med.nyu.edu)

Accepted 9 January 2002

SUMMARY

Precise temporal and spatial control of transcription is a fundamental component of embryonic development. Regulation of transcription elongation can act as a rate-limiting step during mRNA synthesis. The mechanisms of stimulation and repression of transcription elongation during development are not yet understood. We have identified a class of zebrafish mutations (*pandora*, *sk8* and *s30*) that cause multiple developmental defects, including discrete problems with pigmentation, tail outgrowth, ear formation and cardiac differentiation. We demonstrate that the *pandora* gene encodes a protein similar to Spt6, a proposed transcription elongation factor. Additionally, the *sk8* and *s30* mutations are null alleles of the *foggy/spt5* locus, which encodes another transcription elongation factor. Through real-time RT-PCR analysis, we demonstrate that Spt6 and Spt5 are both required for efficient kinetics of *hsp70* transcription in vivo. Altogether, our results suggest that Spt6 and Spt5 play essential roles of comparable importance for promoting transcription during embryogenesis. This study provides the first genetic evidence for parallel functions of Spt6 and Spt5 in metazoans and establishes a system for the future analysis of transcription elongation during development.

Supplemental figure available on-line

Key words: Heart, Spt6, Spt5, Transcription elongation, Real-time RT-PCR, *hsp70*, Zebrafish

INTRODUCTION

Embryonic differentiation depends upon tissue-specific gene expression programs, created by temporally and spatially regulated transcription. Production of specific mRNAs can be stimulated or repressed via regulation of transcription initiation. Transcript production can also be controlled through a rate-limiting step of transcription elongation (Lis, 1998). For example, heat shock response genes, such as *hsp70*, are constitutively occupied by a RNA polymerase II (Pol II) complex that is paused proximal to the promoter after transcription initiation (Rougvie and Lis, 1988; Rasmussen and Lis, 1993). Transcription elongation is inhibited until heat shock stimulation occurs, at which time the paused Pol II becomes hyperphosphorylated and transcript synthesis proceeds. Several factors have been implicated in the stimulation or repression of transcription elongation (Conaway et al., 2000; Winston, 2001; Yamaguchi et al., 2001; Zorio and Bentley, 2001), but their precise regulatory roles during development remain elusive.

Genetic analysis in yeast provided the first indication that the factors Spt4, Spt5 and Spt6 could regulate transcription elongation (Winston et al., 1984; Swanson and Winston, 1992; Bortvin and Winston, 1996; Hartzog et al., 1998). Biochemical studies demonstrated that Spt4 and Spt5 form a physical complex, known as DSIF (DRB sensitivity inducing factor), that interacts with Pol II (Hartzog et al., 1998; Wada et al., 1998). The DSIF complex is involved with both stimulation and repression of transcription elongation in vitro. For example, in an in vitro assay with limiting nucleotide concentrations, addition of DSIF stimulates elongation; by contrast, under different experimental conditions, DSIF is required for the repression of elongation by the inhibitor DRB (5,6-dichloro-1-β-D-ribofuranosylbenzimidazole) (Wada et al., 1998).

Specific in vivo contexts may involve either the stimulatory function or the repressive function of the Spt4/Spt5 complex. During HIV infection, Tat-dependent transactivation of viral transcription requires DSIF for the progress of transcription elongation (Wu-Baer et al., 1998; Garber and Jones, 1999). A stimulatory role for the Spt4/Spt5 complex has also been suggested by the observation that Spt5 is located at sites of

active transcription on *Drosophila* polytene chromosomes and is recruited to heat shock loci upon heat shock stimulation (Andrulis et al., 2000; Kaplan et al., 2000). Repressive functions of the Spt4/Spt5 complex may also be important in vivo. A zebrafish mutation (*foggy*^{m806}) that inhibits the development of dopaminergic neurons has been shown to alter one amino acid (V1012D) in the C terminus of the zebrafish Spt5 protein (Guo et al., 2000). Biochemical analysis of the *foggy*^{m806} mutant Spt5 protein indicates that its repressive function is reduced, but its stimulatory function is unaffected, suggesting that Spt4/Spt5-mediated repression of transcription elongation regulates neuronal development. Although these studies suggest that the Spt4/Spt5 complex has multiple important roles in vivo, the developmental consequences of a complete loss of function of Spt4 or Spt5 have not yet been analyzed.

Spt6 is often considered together with Spt4 and Spt5, as mutations of all three genes cause similar phenotypes in yeast (Winston et al., 1984; Swanson and Winston, 1992; Hartzog et al., 1998). However, the biochemical properties of Spt6 are distinct from those of Spt4 and Spt5. Spt6 is not tightly bound to the Spt4/Spt5 complex (Hartzog et al., 1998), and, unlike Spt4 and Spt5, Spt6 binds to histones, particularly histone H3 (Bortvin and Winston, 1996). Furthermore, Spt6 can assemble nucleosomes on a plasmid template in vitro, and yeast *spt6* mutations can cause alterations in chromatin structure similar to those caused by mutations in histone genes (Bortvin and Winston, 1996). Altogether, these data suggest that Spt6 could regulate transcription by modulating chromatin assembly.

The roles of Spt6 during transcription elongation have not been studied in as much detail as the roles of the Spt4/Spt5 complex. Like Spt4 and Spt5, Spt6 may stimulate transcription elongation: in *Drosophila*, Spt6 colocalizes with Spt5 at sites of active transcription and is recruited to heat shock loci upon heat shock stimulation (Andrulis et al., 2000; Kaplan et al., 2000). Spt6 may also function to repress transcriptional progress: in yeast, mutation of *spt6* suppresses the repression of *SUC2* transcription caused by a *snf5* mutation (Bortvin and Winston, 1996). Thus, Spt6 could potentially play either a stimulatory or a repressive role during development. In the *C. elegans* embryo, *emb-5*, which encodes a Spt6-like protein, interacts genetically with the Notch pathway (Hubbard et al., 1996). Furthermore, EMB-5 can interact physically with Notch, and so EMB-5 may facilitate transcriptional responses to Notch signaling (Hubbard et al., 1996). Overall, the exact functions of Spt6 in vivo, and how they relate to the functions of the Spt4/Spt5 complex, are not yet clear.

Direct comparison of the effects of disabling the Spt4/Spt5 complex and the effects of disabling Spt6 could clarify the roles of these factors. We describe a class of zebrafish mutations (*pandora*, *sk8* and *s30*) that cause similar embryonic phenotypes. We demonstrate that the *pandora* gene encodes a zebrafish Spt6 protein, and that the *sk8* and *s30* mutations are null alleles of the *foggy/spt5* locus. Furthermore, using both a heat-inducible reporter transgene and quantitative real-time RT-PCR, we show that both Spt6 and Spt5 are necessary for efficient kinetics of the transcriptional response to heat shock stimulation. These data provide the first genetic evidence for parallel stimulatory functions of Spt6 and Spt5 in metazoan transcription. Furthermore, this study demonstrates the importance of the precise control of transcriptional kinetics for proper embryogenesis.

MATERIALS AND METHODS

Zebrafish and embryos

Zebrafish and embryos were maintained at 28°C and staged as previously described (Westerfield, 1995). *pan*^{m313}, *fog*^{s30} and *fog*^{sk8} are recessive embryonic lethal mutations that segregate in a Mendelian fashion. Mutant embryos were generated by mating adult heterozygotes or double heterozygotes. The *sk8* mutation was identified during a screen for ethylnitrosourea-induced mutations that disrupt cardiogenesis (D. H. L., A. Schier, and D. Y., unpublished). The *s30* mutation arose spontaneously in the Princeton University zebrafish colony and was identified during routine intercrosses. *sk8* and *s30* fail to complement each other: when crossing a *sk8* heterozygote to a *s30* heterozygote, 24.4% (133/545) of the progeny display the mutant phenotype.

In situ hybridization

Whole-mount in situ hybridization was carried out as previously described (Yelon et al., 1999). An antisense *spt6* probe was generated from a 1534 bp fragment of *spt6* cDNA (beginning at nucleotide 2425). An antisense *spt5* probe was generated from a full-length *spt5* EST (fb16g03; http://zfish.wustl.edu).

Photography

Embryos were viewed with Zeiss Axioplan and Zeiss M2Bio microscopes and photographed with a Zeiss Axiocam digital camera. Images were processed using Zeiss Axiovision and Adobe Photoshop software.

Linkage analysis

To map mutations, heterozygous females were bred to wild-type males from the polymorphic strain Wik, and the progeny of these crosses were raised to adulthood. Heterozygous females from the new lines were used to generate gynogenetic haploids or diploids (Westerfield, 1995). Genomic DNA preps, bulk segregant analysis, and half-tetrad analysis were performed as previously described (Talbot and Schier, 1999; Yelon et al., 2000). Markers for linkage analysis were identified on current maps of the zebrafish genome:
http://zebrafish.mgh.harvard.edu/mapping/ssr_map_index.html;
http://zebrafish.stanford.edu/genome/Frontpage.html;
http://zfish.wustl.edu;http://wwwmap.tuebingen.mpg.de/;
http://mgchd1.nichd.nih.gov:8000/zfrh/current.html; and
http://134.174.23.167/zonrhmapper/Maps.htm.
Fragment length polymorphisms were detected on agarose gels and single-stranded conformational polymorphisms (SSCP) were detected on acrylamide gels (Shimoda et al., 1999; Fornzler et al., 1998). SSCP PCR primers were 5′-TTTCTGAAGATGTTCACCGTCTAA-3′ and 5′-GTTTTGTTTTCCAGTTCAAATCCT-3′ for the 3′ UTR of *spt6*, and 5′-GCTTCTGGCAGAGACACACC-3′ and 5′-ACAACTAA-GCAGTTAATCATTCTGAGG-3′ for the *pan* mutation.

Cloning of zebrafish *spt6* cDNA

Total RNA was extracted from wild-type embryos using Trizol (Life Technologies). Reverse transcription and 5′ RACE were performed using the SMART RACE cDNA amplification system (Clontech). RACE primers were based on the fj42h11.y1 EST sequence. PCR products were sequenced using an ABI Prism 377 apparatus. Sequence analysis was performed using NCBI BLAST algorithms and Lasergene (DNASTAR) software. Sequence was confirmed in at least three independent amplifications of each region of cDNA. The GenBank Accession Number for zebrafish *spt6* is AF421378.

Identification of mutations in cDNA and genomic DNA

cDNA and genomic DNA were generated from wild-type embryos and mutants as previously described (Yelon et al., 2000). Regions of cDNA and genomic DNA were PCR amplified and sequenced, and sequences were confirmed in at least three independent amplifications.

PCR primers used were for the mis-spliced region of *spt6* (Fig. 2A) (5′-GCTTCTGGCAGAGACACACC-3′ and 5′-AGCCGTCCAGAACTTCAATGT-3′), the 5′ region of *spt5* (Fig. 3A) (5′-GGAAGAACAGGGAAGTGTAGCCGGC-3′ and 5′-CATCCAAGATGAAGCCACCATGTCG-3′), the 3′ region of *spt5* (Fig. 3A) (5′-CGTGAAGAGGAATTCCATTGTTAT-3′ and 5′-ACCTTTAATGTGCTCAGTCAG-3′) and the mis-spliced region of *spt5* (Fig. 3B) (5′-GATGACATCACACAGCAACAATTGC-3′ and 5′-ACAAGTGAATTTGCTGTAGGTTTG-3′).

Microinjection of mRNAs and morpholinos

Expression constructs were generated by subcloning either the *spt6* or *spt5* ORF into pCS2. The *spt6*^{m313} mutant construct was generated by replacing a 375 bp fragment of pCS2-*spt6* with a 466 bp fragment amplified from *pan*^{m313} cDNA. To generate the *spt5*^{sk8} mutant construct, the first 609 bp of the ORF in pCS2-*spt5* were replaced with the first 578 bp of the ORF amplified from *fog*^{sk8} cDNA. Capped synthetic mRNA was generated from expression constructs using the SP6 mMessage mMachine system (Ambion). The *spt6* morpholino sequence was: 5′-CCTCGCTCTCGATGAAGTCAGACAT-3′ (GeneTools). Embryos were microinjected at the one-cell or two-cell stage with 50-100 pg of mRNA or 3 ng of morpholino.

Genotyping

Embryos were genotyped after in situ hybridization, mRNA injection or heat shock treatment as necessary. Genomic DNA was extracted from individual embryos as previously described (Yelon et al., 2000). *pan*$^{+/+}$, *pan*$^{m313/+}$ and *pan*$^{m313/m313}$ embryos could be distinguished by a SSCP polymorphism generated by the *pan*^{m313} point mutation. *fog*$^{s30/s30}$ embryos could be detected using multiplex PCR to amplify a region of *spt5* genomic DNA and a positive control region of genomic DNA simultaneously (Fig. 3A). PCR primers included those described above and positive control primers from the 3′ UTR of EST fj20e05 (http://zfish.wustl.edu): 5′-CCATCATCAAGTTCCCCTTG-3′ and 5′-GCAACATCCCATGCATCATA-3′. PCR primers used to detect the *hsp70-egfp* transgene were 5′-TCCGGAGCCACCATGGTGAGCAAGGGCGAGG-3′ and 5′-GGTCGGGGTAGCGGCTGAAGCACTGCACGCC-3′.

Analysis of *hsp70-egfp* transgenics

Fish carrying the stably integrated *hsp70-egfp* reporter transgene (Halloran et al., 2000) were bred to *fog*^{s30}*;pan* double heterozygotes. The progeny were raised and adult fish heterozygous for the *hsp70-egfp* transgene and either or both of *fog*^{s30} and *pan* were identified. These fish were mated with heterozygotes for either or both of *fog*^{s30} and *pan*. The resulting embryos were heat shocked via transfer to embryo medium prewarmed to 37°C. After 1 hour, embryos were cooled to 28°C. Embryos were photographed 30 minutes after the completion of heat shock. Embryonic genotypes were confirmed after photography.

Analysis of *hsp70* induction using real-time RT-PCR

Embryos were grown until 18.5 hpf (19-somite stage) and heat shocked as described above. From each clutch, a set of three mutants and a set of three wild-type siblings were flash-frozen at each time point (0, 10, 20, 30, 40 and 60 minutes after initiation of heat shock). Total RNA was extracted using Trizol and treated with DNAse. First-strand cDNA was reverse transcribed using oligo-dT primers and Superscript reverse transcriptase (Life Technologies). For amplification of *hsp70* and *β-actin*, PCR primers used were 5′-CAACAACCTGCTGGGCAAA-3′ and 5′-GCGTCGATGTCGAAGGTCA-3′ for *hsp70* (AF006007); and 5′-CGAGCAGGAGATGGGAACC-3′ and 5′-CAACGGAAACGCTCATTGC-3′ for *β-actin* (AF057040). Primers were tested using conventional PCR and shown to amplify a single band of approximately 100 bp without production of primer dimers. Real-time PCR, which quantifies the amount of product after each cycle, was carried out on each cDNA sample using an i-cycler (BioRad). Each reaction (30 μl) contained 3 μl of cDNA, 15 μl of 2×SYBR Green Master Mix (ABI) and primers at a final concentration of 100 ng/μl. Reactions were heated to 50°C for 2 minutes followed by 95°C for 10 minutes. Subsequently, the reactions proceeded through 50 cycles at 95°C for 10 seconds and 60°C for 1 minute. The fluorescence level (a quantification of product) was determined after each cycle, allowing the detection of the log phase of amplification. i-cycler software was used to define the cycle in which each sample attained the threshold value of fluorescence. The average *β-actin* threshold cycle value was very consistent between preparations. Mean *β-actin* threshold cycle value and standard deviation for each genotype including all time points were 22.96±0.94 (wild type); 22.79±0.50 (*pan*); 22.31±0.53 (*fog*); and 22.42±0.80 (*fog;pan*). To account for small variations between preparations, the *hsp70* threshold cycle value was compared with the corresponding *β-actin* threshold cycle value for each sample. Furthermore, the level of *hsp70* transcript detected was compared with the baseline level detected at time zero to indicate the degree of *hsp70* induction. The equation used to calculate the relative amount of *hsp70* induction was:

$$\text{relative induction} = \frac{2^{-(\text{HX}-\text{AX})}}{2^{-(\text{H0}-\text{A0})}}$$

where HX is the *hsp70* threshold cycle value at time X, AX is the *β-actin* threshold cycle value at time X, H0 is the *hsp70* threshold cycle value at time 0, and A0 is the *β-actin* threshold cycle value at time 0. According to this equation, *hsp70* levels at time 0 were set to a value of 1. *hsp70* levels relative to *β-actin* at time 0 were very consistent between genotypes. Specifically, the average values (with standard deviation) of $2^{-(\text{H0}-\text{A0})}$ were: 0.136±0.010 (wild type); 0.143±0.021 (*pan*); 0.140±0.015 (*fog*); 0.144±0.025 (*fog;pan*). For both *hsp70* and *β-actin*, no-RT controls and water controls gave similar high threshold cycle values, demonstrating that contamination contributed to less than 0.1% of quantified product.

RESULTS

The *pandora*, *sk8* and *s30* mutations cause similar embryonic defects

The *pandora*^{m313} (*pan*) mutation was originally identified during a large-scale screen for mutations affecting zebrafish embryogenesis (Driever et al., 1996). Embryos that are homozygous for the *pan* mutation exhibit several developmental defects, including reduced pigmentation, limited tail growth and small ears (Fig. 1A,B) (Malicki et al., 1996). Additionally, *pan* mutants have a reduced number of myocardial cells, with an especially significant reduction in the number of ventricular myocardial cells (Stainier et al., 1996; Yelon et al., 1999). As a result, *pan* mutants fail to establish circulation and exhibit pericardial edema (Fig. 1A,B).

We identified two new mutations, called *sk8* and *s30*, that are phenotypically similar to *pan* (Fig. 1C,D). Like *pan*, *sk8* and *s30* cause several abnormalities, including pigmentation, tail, ear and cardiac defects. *sk8* and *s30* fail to complement each other (see Materials and Methods), indicating that these mutations affect the same locus. *sk8* homozygotes, *s30* homozygotes and *sk8/s30 trans* heterozygotes display similarly potent phenotypes (data not shown); hereafter, only the *s30* mutant phenotype will be depicted.

While morphological aspects of the *pan* and *s30* mutant phenotypes are very obvious by 36 hours post-fertilization (hpf) (Fig. 1A-D), mutants appear morphologically normal until mid-somitogenesis (17-18 hpf), when they begin to

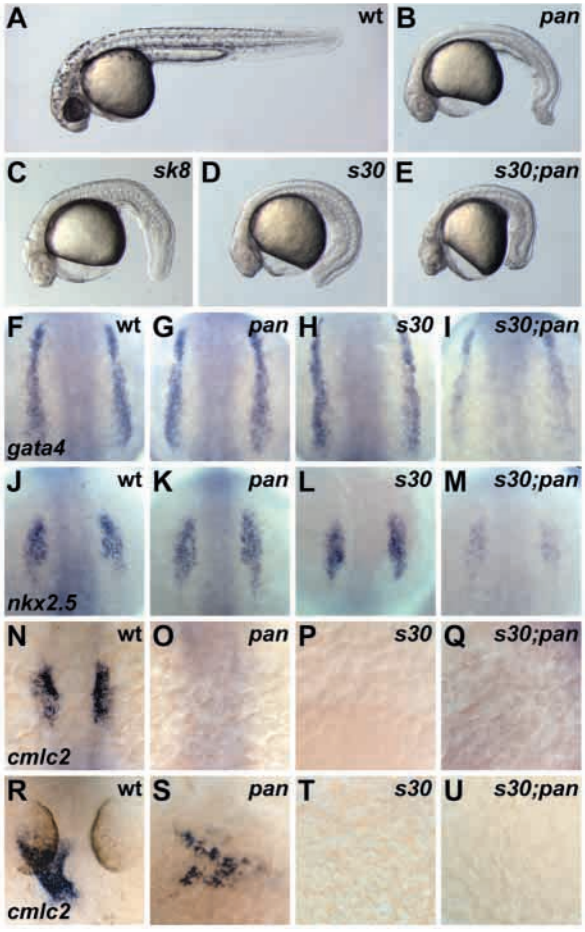

Fig. 1. Morphological and molecular defects are similar among a class of zebrafish mutants. (A-E) Lateral views of live embryos at 36 hours post-fertilization (hpf), anterior towards the left. All embryos are depicted at the same magnification. Compared with wild-type embryos (A), *pan* (B), *sk8* (C) and *s30* (D) mutants exhibit reduced pigmentation, short tails, small ears and pericardial edema. *s30;pan* double mutants (E) exhibit a more extreme phenotype, including a shorter tail and neural cell death. (F-U) Whole-mount in situ hybridization indicates expression of *gata4* (F-I), *nkx2.5* (J-M) or *cmlc2* (N-U); dorsal views of embryos, anterior towards the top. At 13 hpf (eight-somite stage), expression of *gata4* and *nkx2.5* are comparable in wild-type embryos (F,J), *pan* mutants (G,K) and *s30* mutants (H,L); however, expression is reduced in *s30;pan* double mutants (I,M). At 16.5 hpf (15-somite stage), wild-type embryos (N) exhibit robust expression of *cmlc2* in differentiating myocardiocytes, but *pan* mutants (O), *s30* mutants (P) and *s30;pan* double mutants (Q) all lack *cmlc2* expression. By 26 hpf, wild-type embryos (R) form a *cmlc2*-expressing heart tube, and *pan* mutants (S) generate a small and variable number of disorganized myocardiocytes (Yelon et al., 1999), but *cmlc2* remains undetectable in *s30* mutants (T) and *s30;pan* double mutants (U).

display subtly shorter tails than their wild-type siblings (data not shown). To further investigate the earliest requirements for *pan* and *s30*, we focused our attention on the cardiac phenotype. Myocardial cells arise from bilateral populations of anterior lateral plate mesoderm that express *gata4* and *nkx2.5* (Serbedzija et al., 1998; Chen and Fishman, 1996). Initial expression of *gata4* and *nkx2.5* appears normal in *pan* mutants and *s30* mutants (Fig. 1F-H,J-L). However, terminal myocardial differentiation is dramatically inhibited: *pan* mutants and *s30* mutants fail to express the myocardial gene *cmlc2* (Yelon et al., 1999) at 16.5 hpf (Fig. 1N-P). *s30* mutants never generate significant numbers of myocardial cells, but *pan* mutants can generate a small number of disorganized myocardiocytes by 26 hpf (Fig. 1R-T) (Yelon et al., 1999). These phenotypes suggest that the *pan* and *s30* gene products are both required for the normal differentiation of precardiac mesoderm into myocardial tissue.

To investigate the genetic relationship between *pan* and *s30*, we examined embryos homozygous for both mutations. *s30;pan* double mutants exhibit a more extreme phenotype than either *pan* or *s30* mutants (Fig. 1E). Notably, double mutants have a greater reduction in tail length and a significant amount of neural cell death. In addition, *s30;pan* double mutants exhibit a more dramatic cardiac phenotype than either *pan* or *s30* mutants. Specifically, *s30;pan* double mutants exhibit reduced expression of *gata4* and *nkx2.5* (Fig. 1I,M). Predictably, *s30;pan* double mutants fail to generate any differentiated myocardial tissue (Fig. 1Q,U). Overall, the *pan*, *s30* and *s30;pan* mutant phenotypes suggest that the *pan* and *s30* gene products have related functions and that they cooperate during several developmental processes.

Identification of candidate genes on the zebrafish genome map

In order to identify the genes encoded by the *pan* and *s30* loci, we mapped both mutations using half-tetrad analysis and bulk segregant analysis (Talbot and Schier, 1999). We mapped *pan* to a <1 cM interval between the SSLP markers Z21106 (two recombinants in 505 meioses) and Z10567 (12 recombinants in 2282 meioses) on zebrafish linkage group 21. We mapped *s30* to a <1 cM interval between the SSLP markers Z7871 (four recombinants in 587 meioses) and Z20993 (one recombinant in 587 meioses) on zebrafish linkage group 15.

Hypothesizing that *pan* and *s30* play similar roles, we examined the *pan* and *s30* intervals on current maps of the zebrafish genome (see Materials and Methods), focusing on mapped genes that might have similar functions. In the *s30* interval, we found the previously described zebrafish gene *foggy/spt5*, predicted to encode a transcription elongation factor (Guo et al., 2000). In the *pan* interval, we identified an EST (fj42h11; http://zfish.wustl.edu) that is predicted to encode a partial protein with similarity to Spt6, another transcription elongation factor. We then pursued *spt6* and *spt5* as candidates for the genes affected by the *pan* and *s30* mutations, respectively.

The *pan* locus encodes Spt6

Using a polymorphism located within the 3′ UTR of the fj42h11 EST, we determined that fj42h11 was tightly linked to the *pan* mutation (0 recombinants in 1652 meioses). We then used 5′ RACE to clone a complete cDNA corresponding to fj42h11. Sequence analysis revealed a 5178 bp open reading frame (ORF) (Fig. 2B), predicted to encode a protein similar to the human, mouse, *Drosophila*, *C. elegans* and yeast Spt6 proteins (Table 1). All of these Spt6 homologs have similar amino acid sequences, including an acidic N-terminal region, a S1-type RNA binding domain, and a SH2 domain (Table 1, Fig. 2D). Based on these sequence comparisons, we hereafter refer to this zebrafish gene as *spt6*.

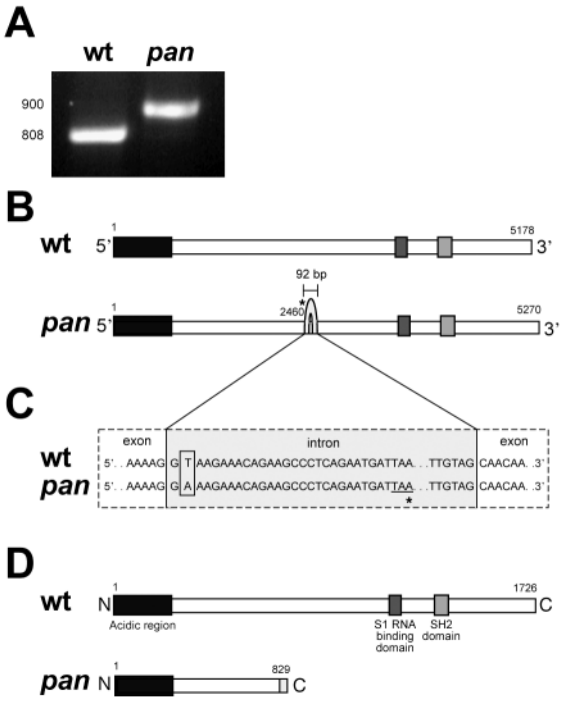

Fig. 2. The *pan*^{m313} mutation causes mis-splicing of *spt6* mRNA and truncation of Spt6 protein. (A) *spt6* cDNA from *pan* mutants at 30 hpf contains a 92 nucleotide insertion. PCR primers that flank an 808 bp fragment of wild-type *spt6* cDNA amplify a 900 bp fragment from *pan* mutant cDNA. This larger fragment represents the major splice isoform of *spt6* in *pan* mutants, although we have infrequently detected trace amounts of normally spliced cDNA that could represent a low level of maintained maternal mRNA or a low level of normal splicing of zygotic mRNA. (B) Comparison of wild-type and *pan* mutant *spt6* cDNA. Labeled regions in the wild-type ORF are proposed to encode discrete protein domains (see D below). The 92 nucleotide insertion in *pan* mutant cDNA is indicated by a loop, and the location of the in-frame stop codon is marked with an asterisk. (C) Genomic sequence of exon-intron boundaries flanking the mutated intron. The insertion in *pan* mutant cDNA corresponds to a 92 bp intron. *pan* genomic DNA contains a point mutation (boxed) in the second nucleotide of this intron. This mutation prevents correct splicing at this junction in *pan* mutants. The in-frame stop codon is underlined and marked with an asterisk. (D) Predicted protein structure for wild-type Spt6 protein (1726 amino acids) and truncated *pan* mutant Spt6 protein (829 amino acids). The acidic region, S1 RNA binding domain and SH2 domain are indicated. The insertion of intronic sequence in *pan* mutant cDNA is predicted to result in the addition of nine mis-sense amino acids before reaching a premature in-frame stop codon. Therefore, the *pan* mutant Spt6 protein would lack both the S1 RNA binding domain and SH2 domain.

Examination of *spt6* cDNA sequence from *pan* mutants revealed that the *pan* mutant cDNA is larger than the wild-type cDNA, owing to an insertion of 92 nucleotides following nucleotide 2460 (Fig. 2A,B). Analysis of *spt6* genomic DNA indicated that this insertion corresponds to the intron that is normally spliced out between nucleotides 2460 and 2461 of the wild-type *spt6* mRNA (Fig. 2C). In *pan* mutant cDNA and genomic DNA, we detected a T-to-A transversion in the second nucleotide of this intron (Fig. 2C). This point mutation is tightly linked to the *pan* mutant phenotype (0 recombinants in 2282 meioses). A conserved T is found in the second intronic nucleotide of all eukaryotic splice donor sites (Padgett et al., 1986). Thus, the *pan* mutation is predicted to inhibit splicing at this junction, consistent with the sequence of the *pan* mutant *spt6* cDNA. Owing to an in-frame stop codon located within the insertion, the *pan* mutant *spt6* cDNA is predicted to produce a truncated Spt6 protein that is unlikely to retain normal function (Fig. 2C,D). To confirm that reduction of Spt6 activity causes the *pan* mutant phenotype, we inhibited Spt6 translation in vivo using an antisense morpholino (Summerton and Weller 1997; Nasevicius and Ekker, 2000) directed against *spt6*. Injection of the anti-*spt6* morpholino produced a phenocopy of the *pan* mutation (see on-line supplemental data). These data indicate that the *pan* locus encodes Spt6.

Table 1. Comparison of Pandora/Spt6 with other Spt6 proteins

Protein	Total protein	S1 RNA-binding domain	SH2 domain
Human SUPT6H GI:1136386	87%/79%	90%/87%	97%/93%
Mouse Supt6h GI:1401057	86%/78%	90%/87%	95%/91%
Drosophila SPT6 GI:6491997	64%/47%	74%/51%	78%/64%
C. elegans EMB-5 GI:285695	56%/36%	62%/37%	71%/45%
Yeast Spt6p GI:172682	44%/25%	61%/33%	67%/40%

Zebrafish Spt6 is most closely related to mammalian Spt6. Percentages represent the amino acid similarity/identity between zebrafish Spt6 and other Spt6 proteins, as determined by alignments using NCBI BLASTp. Comparisons of the total protein sequence, the S1 RNA-binding domain (amino acids 1218-1273 in zebrafish) and the SH2 domain (amino acids 1323-1409 in zebrafish) are provided. The N-terminal acidic domain is also conserved in all Spt6 proteins. In zebrafish, 42% of the first 239 amino acids of Spt6 are aspartic or glutamic acid; a similar percentage of acidic residues are found in the first 239 amino acids of other Spt6 proteins (42% in human, 43% in mouse, 38% in *Drosophila*, 40% in *C. elegans* and 35% in yeast).

The *s30* and *sk8* mutations are null alleles of *foggy/spt5*

Similar to our analysis of *spt6* as a candidate gene for *pan*, we looked for mutations in *spt5* cDNA and genomic DNA in *s30* and *sk8* mutants. PCR analysis of genomic DNA indicated that the entire *spt5* gene is deleted in *s30* mutants (Fig. 3A). This deletion is tightly linked to the *s30* mutant phenotype (0 recombinants in 587 meioses). Thus, *s30* is a deficiency allele of *foggy/spt5*, but the deletion may also remove neighboring genomic DNA. By contrast, the *sk8* mutation causes a lesion specific to *spt5*. Examination of *spt5* cDNA sequence from *sk8* mutants revealed that the *sk8* mutant cDNA is smaller than the wild-type cDNA, with 31 nucleotides missing after nucleotide 520 (Fig. 3B,C). Analysis of *spt5* genomic DNA indicated that this omission corresponds to a 31 bp exon (Fig. 3D). In *sk8* mutant genomic DNA, we detected a point mutation (G-to-A transition) in the first nucleotide of the intron following this small exon (Fig. 3D). This mutation affects a nucleotide that is conserved in all splice donor sites (Padgett et al., 1986). Thus, splicing is inhibited at the mutated junction, evidently leading to the removal of an entire exon. This splicing error produces a frameshift in the *sk8* mutant *spt5* cDNA, and, owing to an in-frame stop codon 30 nucleotides downstream of the frameshift, this cDNA is predicted to produce a truncated Spt5 protein (Fig. 3E). The predicted *sk8* mutant Spt5 protein lacks all KOW motifs (predicted to bind to Pol II) and hexapeptide repeats (predicted to be phosphorylation sites), and is unlikely

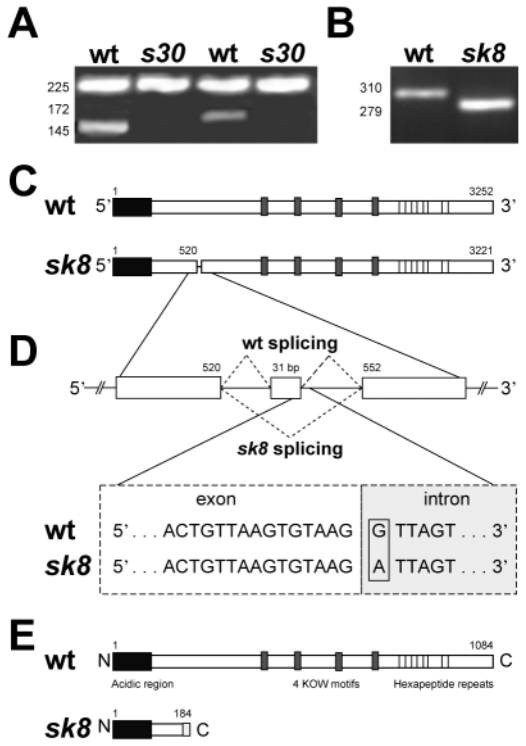

Fig. 3. The *s30* and *sk8* mutations disrupt the *foggy/spt5* locus. (A) The *s30* mutation deletes *spt5*. The first and second lanes demonstrate that a 145 bp fragment of the 5′ end of *spt5* genomic DNA can not be amplified by PCR from *s30* genomic DNA. The third and fourth lanes demonstrate a similar result for a 172 bp fragment of the 3′ end of *spt5* genomic DNA. Similar results were obtained for all regions of *spt5* genomic DNA (data not shown). A control fragment (225 bp) can be amplified from all samples. (B) *spt5* cDNA from *sk8* mutants is missing 31 bp. PCR primers that flank a 310 bp fragment of wild-type *spt5* cDNA amplify a 279 bp fragment from *sk8* mutant cDNA. This smaller fragment represents the major splice isoform of *spt5* in *sk8* mutants at 24 hpf, although we have infrequently detected trace amounts of normally spliced cDNA that could represent a low level of maintained maternal mRNA or a low level of normally spliced mutant mRNA. (C) Comparison of wild-type and *sk8* mutant *spt5* cDNA. Labeled regions are proposed to encode discrete protein features (see E). The location of the missing nucleotides is indicated following nucleotide 520 in *sk8* mutant cDNA. (D) Structure of *spt5* genomic DNA indicates that the missing bases correspond to a 31 bp exon, flanked by a 88 bp intron and a 103 bp intron. In wild-type embryos, this region is spliced normally and the 31 bp exon is located between nucleotides 520 and 552 in *spt5* cDNA. In *sk8* mutants, incorrect splicing results in the omission of the exon and both introns from *spt5* cDNA. *sk8* genomic DNA contains a point mutation (boxed) in the first nucleotide of the intron following the 31 bp exon. (E) Predicted protein structure for wild-type Spt5 protein (1084 amino acids) and truncated *sk8* mutant Spt5 protein (184 amino acids). The acidic region, KOW motifs, and hexapeptide repeats are indicated (Guo et al., 2000). The omission of an exon in *sk8* mutant cDNA creates a frameshift that is predicted to result in the addition of 10 mis-sense amino acids after residue 174 before reaching a premature in-frame stop codon. Therefore, the *sk8* mutant Spt5 protein would lack all KOW motifs and hexapeptide repeats.

to retain normal function. These genetic data indicate that the *s30* and *sk8* mutations are alleles of the previously described *foggy* (*fog*) locus (Guo et al., 2000). Furthermore, as fog^{s30} is a deficiency and $fog^{sk8/s30}$ *trans* heterozygotes are phenotypically identical to $fog^{s30/s30}$ homozygotes (data not shown), both fog^{s30} and fog^{sk8} appear to be null alleles. By contrast, the previously identified hypomorphic allele fog^{m806} is a mis-sense mutation that alters a residue in the C-terminus of Spt5 (V1012D) and leaves significant aspects of Spt5 function intact (Guo et al., 2000).

Overexpression of *spt6* and *spt5* can rescue respective mutant phenotypes

To provide additional confirmation of the genes disrupted by the *pan*, *s30* and *sk8* mutations, we examined the effects of overexpressing *spt6* and *spt5*. Injection of synthetic *spt6* mRNA at the one-cell stage can rescue the *pan* mutant phenotype (Fig. 4A-H; Table 2). Similarly, injection of synthetic *spt5* mRNA can rescue the *fog* mutant phenotype (Fig. 4I-P; Table 2). In both cases, overexpression of synthetic mRNA restores normal pigmentation, tail length, ear formation and cardiac function to mutants without affecting the development of wild-type siblings (Fig. 4; Table 2). Examination of *cmlc2* expression confirmed that myocardial differentiation occurs efficiently in rescued embryos (Fig. 4E-H,M-P). Injection of $spt6^{m313}$ mutant mRNA fails to rescue the *pan* mutant phenotype, and injection of $spt5^{sk8}$ mutant mRNA fails to rescue the *fog* mutant phenotype, verifying that the mutant gene products are nonfunctional (Table 2). Injection of *spt5* mRNA can not rescue *pan* mutants, and injection of *spt6* mRNA can not rescue *fog* mutants (Table 2). Altogether, these data confirm that inactivation of Spt6 and Spt5 are responsible for the *pan* and *fog* mutant phenotypes, respectively.

spt6 and *spt5* are expressed maternally and zygotically

Previous studies of *spt5* expression in zebrafish indicated its broad distribution throughout the embryo from 10 hpf onwards (Guo et al., 2000). We extended this analysis by comparing the expression patterns of *spt6* and *spt5*. At early stages, both transcripts are supplied maternally and found throughout the blastoderm (Fig. 5A,D). After the initiation of zygotic transcription, the expression of both genes remains ubiquitous (Fig. 5B,E). By 24 hpf, *spt6* and *spt5* expression levels are still broad, but are highest in the embryonic brain (Fig. 5C,F).

Zygotic expression of *spt5* is not detectable in fog^{s30} mutants, in accordance with the deletion of *spt5* from fog^{s30} genomic DNA (Fig. 5E, inset). The expression pattern of *spt5* in fog^{s30} mutants indicates that most maternally provided *spt5* mRNA is degraded by 10 hpf (Fig. 5E). Expression of *spt5* and *spt6* in both fog^{sk8} mutants and *pan* mutants is similar to expression in wild-type siblings (data not shown).

Spt6 and Spt5 are required to promote transcriptional response to heat shock

Having established that *pan* and *fog* mutants lack zygotic supplies of Spt6 and Spt5, we were provided with an opportunity to test the roles of these factors during transcription in vivo. First, we generated wild-type and mutant embryos that were heterozygous for a *hsp70-egfp* reporter transgene, a stably integrated construct in which *egfp* expression is controlled by the zebrafish *hsp70* promoter

Table 2. Rescue of mutant phenotypes by respective wild-type mRNA

Genotype	Injected mRNA	% Wild-type embryos
$pan^{m313/+} \times pan^{m313/+}$	Uninjected	75.6 (118/156)
$pan^{m313/+} \times pan^{m313/+}$	*spt6*	96.5 (274/284)
$pan^{m313/+} \times pan^{m313/+}$	$spt6^{m313}$	75.8 (91/120)
$pan^{m313/+} \times pan^{m313/+}$	*spt5*	77.8 (84/108)
$fog^{s30/+} \times fog^{s30/+}$	Uninjected	74.4 (128/172)
$fog^{s30/+} \times fog^{s30/+}$	*spt5*	94.4 (168/178)
$fog^{s30/+} \times fog^{s30/+}$	$spt5^{sk8}$	74.7 (59/79)
$fog^{s30/+} \times fog^{s30/+}$	*spt6*	75.9 (66/87)

pan^{m313} and fog^{s30} mutant phenotypes can be rescued by injection of *spt6* and *spt5* mRNA, respectively. For each experiment, *pan* heterozygotes or *fog* heterozygotes were mated and the resulting clutches were injected with the mRNA indicated. Embryos were scored for pigmentation, body shape, ear formation, heart morphology and blood circulation. When all of these traits were normal, the embryo was scored as having a wild-type phenotype. In each case, injection of the respective wild-type mRNA rescued nearly all of the injected mutants (predicted to be 25% of the embryos in each clutch). Injection of mutant mRNA ($spt6^{m313}$ or $spt5^{sk8}$) did not rescue mutants. *spt5* mRNA did not rescue *pan* mutants and *spt6* mRNA did not rescue *fog* mutants. None of the injected mRNAs affected wild-type siblings (predicted to be 75% of the embryos in each clutch).

(Halloran et al., 2000). When maintained at normal temperature, transgenic wild-type embryos, *pan* mutants, fog^{s30} mutants and fog^{s30}*;pan* double mutants do not produce detectable levels of GFP (Fig. 6A-D), although consistent autofluorescence is visible in the embryonic yolk. We administered a 1 hour heat shock to these embryos beginning at 18.5 hpf, a stage at which we expected minimal maternal contribution of Spt6 or Spt5. After heat shock stimulation, wild-type embryos produce high levels of GFP, but *pan* mutants and fog^{s30} mutants produce only low and less uniform levels of GFP (Fig. 6E-G,I-K). fog^{s30}*;pan* double mutants are more severely affected and do not produce any detectable GFP (Fig. 6H,L). Thus, heat shock response appears to be inefficient in the absence of Spt6 or Spt5 and undetectable in the absence of both proteins.

Inhibition of GFP production in *hsp70-egfp* transgenic embryos could be the result of diminished transcription; alternatively, GFP production could be inhibited post-transcriptionally through modification of transcript stability, translation or protein processing/folding. To determine whether absence of Spt6 and/or Spt5 interferes with the transcriptional response to heat shock, we examined the levels of endogenous *hsp70* mRNA directly, using real-time RT-PCR (see Materials and Methods). We administered a 1 hour heat shock to embryos beginning at 18.5 hpf, the earliest stage at which mutants can be reliably distinguished from their wild-type siblings by subtle morphological criteria. Within 10 minutes of heat shock stimulation, wild-type embryos express 25 times more *hsp70* than they do before heat shock (Fig. 6M). Wild-type expression of *hsp70* peaks at nearly 75 times the basal expression level after 40 minutes of heat shock, in accordance with previous descriptions of the kinetics of *hsp70* induction in zebrafish (Lele et al., 1997). In contrast to the dynamics of wild-type expression, induction of *hsp70* expression in *pan* mutants or fog^{s30} mutants is slow and weak (Fig. 6M). After 10 minutes of heat shock stimulation, *pan* or fog^{s30} mutants express only 15 times more *hsp70* than before heat shock. Additionally, in *pan* or fog^{s30} mutants, the level of *hsp70* induction does not rise more than 21 times over baseline during the course of a 1 hour heat shock. The sensitivity of the real-time RT-PCR assay also revealed that fog^{s30}*;pan* double mutants can generate a weak response to heat shock stimulation, although induction of *hsp70* expression in double mutants is more severely inhibited than in single mutants (Fig. 6M). Therefore, efficient kinetics of the transcriptional response to heat shock depends upon the individual and coordinated functions of Spt6 and Spt5.

DISCUSSION

The zebrafish pan^{m313}, fog^{sk8} and fog^{s30} mutations provide the first opportunity to compare the effects of *spt6* and *spt5* loss-of-function in metazoans. These *pan* and *fog* mutations cause similar embryonic defects, including inhibition of myocardial differentiation. Furthermore, *fog;pan* double mutants have enhanced abnormalities, including earlier defects in the formation of precardiac mesoderm. We have observed the same functional relationship between *pan* and *fog* during the transcriptional response to heat shock stimulation: *pan* mutants and *fog* mutants exhibit similar difficulties with efficient induction of *hsp70*, and *fog;pan* double mutants exhibit more extreme inhibition of *hsp70* induction. Altogether, our genetic analysis indicates that Spt6 and Spt5 play essential roles of comparable importance during development, controlling multiple aspects of differentiation through stimulation of gene expression.

Spt6 and Spt5 promote transcription during heat shock response

Previous studies in *Drosophila* have established that Spt6 and Spt5 colocalize with hyperphosphorylated Pol II at transcriptionally active loci on polytene chromosomes (Andrulis et al., 2000; Kaplan et al., 2000). In particular, both Spt6 and Spt5 are recruited to heat shock genes, including *hsp70*, shortly after the initiation of heat shock. These data suggested that Spt6 and Spt5 could function to promote transcription elongation at heat shock loci. Our data provide genetic evidence in support of this model by demonstrating that the absence of Spt6 or Spt5 significantly affects the efficacy and kinetics of *hsp70* induction.

Our analysis cannot resolve whether Spt6 and Spt5 act directly at the *hsp70* promoter, nor can it resolve whether Spt6 and Spt5 act at the level of transcription elongation per se. It is possible that Spt6 and Spt5 regulate *hsp70* mRNA stability, or that they are responsible for generating other factors required to manifest a heat shock response. However, the zebrafish *hsp70* promoter has significant sequence similarity to characterized heat shock promoters in *Drosophila* (Halloran et al., 2000), and it is therefore reasonable to expect that Spt6 and Spt5 would be present at the zebrafish *hsp70* promoter and could function there directly. In any case, our data clearly indicate that Spt6 and Spt5 act to promote gene expression, possibly via regulation of transcription elongation.

Spt5 and Spt6 seem to be equivalently important for transcriptional efficiency, but their biochemical properties are very different. We have shown that Spt5 can not rescue *pan* mutants and that Spt6 can not rescue *fog* mutants, confirming that these factors can not substitute for each other functionally, as previously demonstrated in yeast (Swanson and Winston,

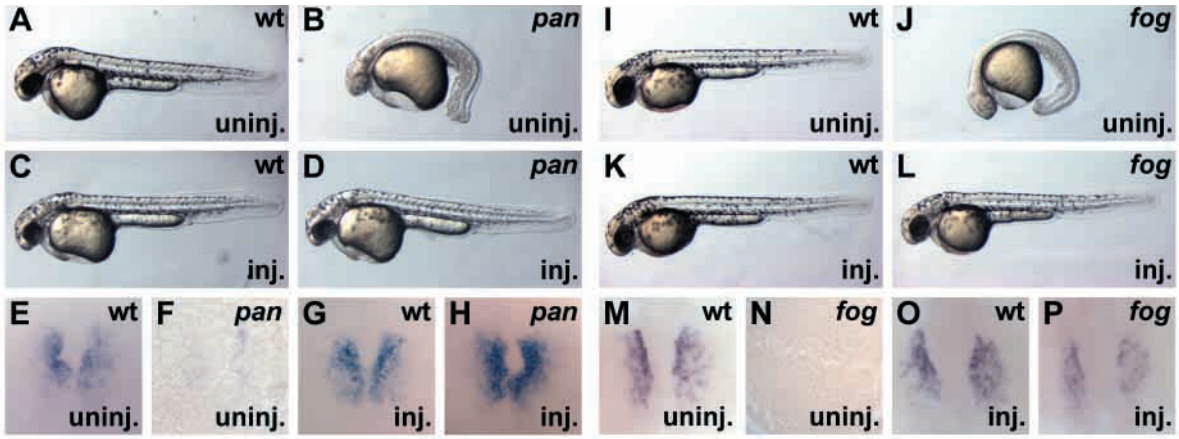

Fig. 4. *spt6* and *spt5* mRNA rescue the defects in *pan* and *fog*^{s30} mutants, respectively. Uninjected embryos (A,B,E,F,I,J,M,N) are compared with embryos that were injected with synthetic mRNA, either *spt6* (C,D,G,H) or *spt5* (K,L,O,P). All embryonic genotypes were confirmed following photography (see Materials and Methods). Genotypes are: wild-type embryos (A,C,E,G,I,K,M,O); *pan* mutants (B,D,F,H); and *fog*^{s30} mutants (J,L,N,P). (A-D,I-L) Lateral views of live embryos at 36 hpf, anterior towards the left. Injection of wild-type mRNA rescues pigmentation, tail length, ear formation and cardiac function in mutants, and does not affect wild-type siblings. Rescued embryos survive for 4-5 days post-fertilization. (E-H,M-P) Whole-mount in situ hybridization indicates expression of *cmlc2* at 16.5-17.5 hpf; dorsal views of embryos, anterior towards the top. Injection of wild-type mRNA rescues the timely and robust expression of *cmlc2* expression in mutants and does not affect expression in wild-type siblings.

1992). Thus, Spt5 and Spt6 are likely to play distinct biochemical roles that both contribute to transcriptional progress. Removal of either Spt5 or Spt6 cripples transcriptional efficiency, and removal of both Spt5 and Spt6 compounds the transcriptional defects. Even so, *hsp70* induction is not completely eliminated in *fog;pan* double mutants. The low levels of *hsp70* in double mutants may be facilitated by residual supplies of maternal Pan or Fog or contributions from other elongation factors, including additional Spt5 or Spt6 homologs. However, there are currently no indications of other zebrafish genes similar to *spt6* or *spt5* in EST or genomic sequence databases (J. L. F., B. R. K. and D. Y., unpublished).

Previous studies have indicated that the Spt4/Spt5 complex can repress transcription elongation in vitro (Wada et al., 1998). Furthermore, colocalization of Spt5 with paused, hypophosphorylated Pol II at heat shock loci in *Drosophila* has suggested that Spt5 could be involved with polymerase pausing (Andrulis et al., 2000; Kaplan et al., 2000). We do not detect a loss of repression (i.e. constitutive activation) of *hsp70* expression in *fog* or *pan* mutants. However, detection of constitutive expression in our RT-PCR assay depends upon the successful production of full-length transcripts. Therefore, evidence in favor of a repressive function of Spt5 could be masked by the requirement for a stimulatory function of Spt5.

Spt6 and Spt5 promote transcription during development

The embryonic phenotypes of *pan* and *fog* mutants indicate that the loss of either Spt6 or Spt5 can cause similar developmental defects. Extrapolating from the activities of Spt6 and Spt5 during *hsp70* induction, it is likely that the *pan* and *fog* mutant phenotypes represent the cumulative effects of inefficient transcription at multiple embryonic loci. For example, myocardial development in zebrafish requires the activity of the transcription factors Gata5 and Hand2 (Reiter et al., 1999; Yelon et al., 2000). In *pan* and *fog* mutants, it is likely that the genes regulated by Gata5, Hand2 and other myocardial transcription factors are inefficiently expressed; thus, terminal myocardial differentiation is inhibited, although precardiac mesoderm forms relatively normally. In *fog;pan* double mutants, transcriptional efficiency is further compromised; thus, myocardial development is affected at an earlier stage, during the formation or

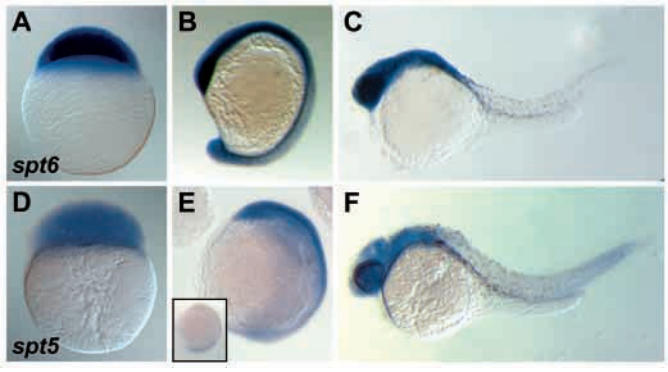

Fig. 5. *spt6* and *spt5* are expressed maternally and zygotically throughout the zebrafish embryo. Whole-mount in situ hybridization, comparing the expression patterns of *spt6* (A-C) and *spt5* (D-F). Wild-type embryos at 2.75 hpf (512-cell) (A) or 2.25 hpf (128-cell) (D) demonstrate that both *spt6* (A) and *spt5* (D) are expressed throughout the blastoderm before the initiation of zygotic transcription and are therefore maternally supplied. (A,D) Lateral views, with the animal pole at the top. Wild-type embryos at 16.5 hpf (B) or 10 hpf (E) demonstrate that *spt6* (B) and *spt5* (E) are expressed throughout the embryo after the initiation of zygotic transcription. Inset in E depicts a *fog*^{s30} mutant embryo at 10 hpf. *spt5* mRNA is barely detectable in *fog*^{s30} mutants at this stage, in keeping with the deletion of *spt5* in *fog*^{s30} mutant genomic DNA. (B,E) Lateral views, anterior towards the top. Wild-type embryos at 24 hpf (C) or 26 hpf (F) demonstrate that *spt6* (C) and *spt5* (F) are still broadly expressed, with highest levels in the embryonic brain. (C,F) Lateral views, anterior towards the left.

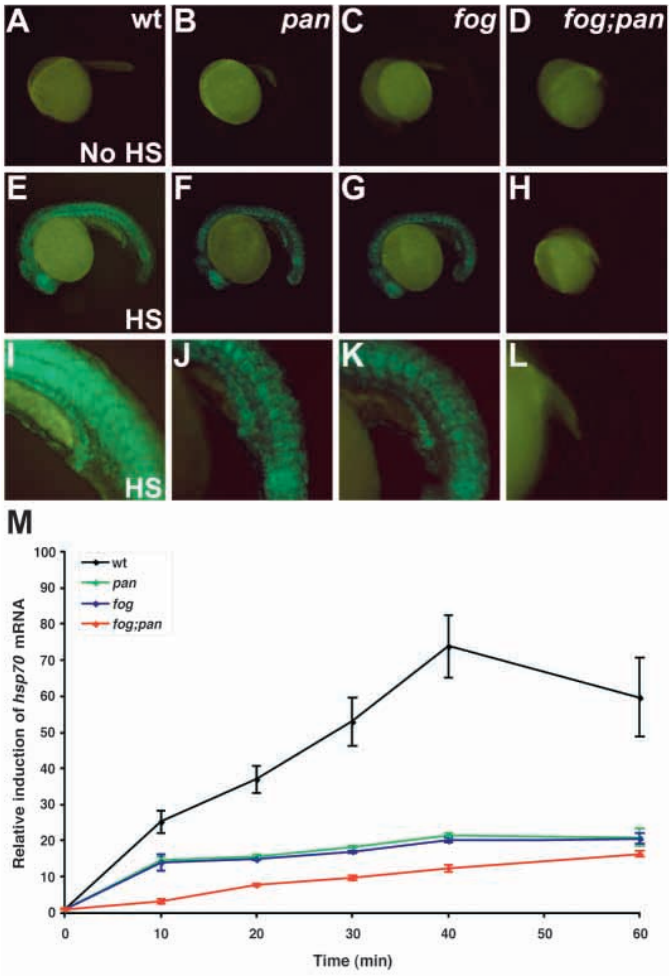

Fig. 6. Spt6 and Spt5 are required for an efficient heat shock response. (A-L) Lateral views of live embryos at 20 hpf (22-somite stage), anterior towards the left. Green fluorescence indicates production of GFP after a 1 hour heat shock and a 0.5 hour recovery period. Autofluorescence (yellow-green) is also visible in embryonic yolks. All photographs were taken with the same exposure time, and embryonic genotypes were confirmed after photography (see Materials and Methods). Genotypes are wild-type embryos (A,E,I); *pan* mutants (B,F,J); *fog*^{s30} mutants (C,G,K); and *fog*^{s30}*;pan* double mutants (D,H,L). All embryos are heterozygous for the *hsp70-egfp* transgene (Halloran et al., 2000). Embryos maintained at normal temperature do not produce detectable GFP (A-D). After heat shock, *pan* and *fog* mutants produce less GFP than wild-type embryos, and double mutants do not produce any detectable GFP (E-H, with higher magnification views of the tail in I-L). Similar results were obtained when heat shock was administered from 15-16 hpf, before mutant phenotypes are morphologically apparent (data not shown). (M) Spt6 and Spt5 are required for efficient induction of *hsp70* expression during a 1 hour heat shock. Graph of induction of endogenous *hsp70* expression, detected by real-time RT-PCR. (See Materials and Methods for details of technique and data processing.) Wild-type embryos (black) induce significantly higher levels of *hsp70* mRNA with more rapid kinetics than *pan* mutants (green) or *fog*^{s30} mutants (blue). *hsp70* induction is further inhibited in *fog*^{s30}*;pan* double mutants (red). Each data point represents the average degree of induction of *hsp70* expression at a particular time point, relative to the low, but detectable, levels of *hsp70* expression at time zero. Standard deviation from the mean is indicated by error bars. To account for small variances in RNA extraction and cDNA synthesis, levels of *hsp70* expression were normalized relative to levels of stable *β-actin* expression (see Materials and Methods).

maintenance of precardiac mesoderm. Similar models can be proposed for other aspects of the mutant phenotypes; however, not every tissue seems to be equally affected by a loss of Spt6 and/or Spt5. For example, *fog;pan* double mutants exhibit normal lens induction at 19.5 hpf and normal touch responses at 24 hpf, even though they are significantly affected in other aspects of differentiation at these stages (B. R. K. and D. Y., unpublished).

Because of the maternal contribution of Spt6 and Spt5, it is difficult for our studies to resolve whether Spt6 and Spt5 are universally required to promote transcription at all zebrafish promoters. Although *pan* and *fog* mutants are significantly abnormal, more severe phenotypes, particularly developmental arrest before gastrulation, can be generated by treating zebrafish embryos with the Pol II inhibitor α-amanitin (Kane et al., 1996) or by morpholino-mediated inhibition of TBP function (Muller et al., 2001). Both of these treatments affect zygotic transcription from its beginning in the embryo. Therefore, we expect that maternally supplied Spt6 and Spt5 permit normal transcription at early stages in *pan* and *fog* mutants, and that the observed phenotypes reflect the roles of zygotic gene products after maternal supplies have been depleted in particular tissues. Further study will be required to determine whether any specific promoters vary in their requirements for Spt6 and Spt5.

Previous studies of the *fog*^{m806} hypomorphic allele have indicated specific roles for the repressive activity of Spt5 during neuronal development in zebrafish (Guo et al., 2000). In vitro assays have indicated that the *fog*^{m806} mutant Spt5 protein has limited repressive function, but retains its stimulatory function. *fog*^{m806} mutants exhibit a significant deficit of dopaminergic neurons at 28 hpf, but have normal body shape, tail length, ear development and heart tube formation, although cardiovascular function appears impaired after 30 hpf (Guo et al., 1999; Guo et al., 2000). By contrast, the mutant phenotypes caused by the null alleles *fog*^{s30} and *fog*^{sk8} are substantially more dramatic and appear earlier than the *fog*^{m806} mutant phenotype. Based on these phenotypic comparisons and our demonstration of the stimulatory role of Spt5 during *hsp70* induction, we propose that the stimulatory role of Spt5 is more widely employed, in a broader range of embryonic tissues, than is its repressive role. This model is consistent with colocalization studies in *Drosophila* that demonstrate preferential association of Spt5 with hyperphosphorylated Pol II rather than paused Pol II (Andrulis et al., 2000; Kaplan et al., 2000).

A system for study of transcription elongation during development

Future studies of zebrafish *pan* and *fog* mutants will allow a more detailed analysis of the precise roles of Spt6 and Spt5 during embryogenesis. In particular, our phenotypic rescue assay will allow detailed structure-function analysis of Spt6 and Spt5 in vivo, facilitating correlation of proposed functional domains (Yamaguchi et al., 1999; Ivanov et al., 2000) with specific roles during embryogenesis. Furthermore, ongoing genetic screens are likely to identify additional mutations in the *pan/fog* phenotypic class. We have already identified a new mutation in this class (*sk11*) that is phenotypically indistinguishable from *fog*^{s30} or

fog^{sk8} and that complements both *pan* and *fog* (D. H. L., A. Schier, and D. Y., unpublished). Thus, the gene disrupted by *sk11* is likely to be another important component of the transcriptional apparatus, perhaps even a novel factor. Altogether, the zebrafish embryo provides unique opportunities for the analysis of transcriptional regulation during embryogenesis.

We thank several people for their contributions to this project, particularly Benson Lu for mapping *pan* between Z10567 and Z21106. We also thank C. Ott for initial work on *pan*; S. Zimmerman, T. Bruno, A. Navarro and S. Waldron for excellent fish care; J. Malicki for *pan* heterozygotes; J. Kuwada for *hsp70-egfp* transgenic fish; R. Yang and B. Baysa for sequencing; N. Tanese, J. Treisman and members of the Schier and Yelon laboratories for helpful discussions; D. Littman, J. Lafaille, M. Lafaille and A. Wensky for help with real-time RT-PCR; and A. Schier for exceptional support and generosity. B. R. K. and D. H. L. are supported by the MSTP of NYU School of Medicine. This work was supported by a Burroughs Wellcome Fund Career Award and a New York City Council Speaker's Fund for Biomedical Research Award to D. Y.

REFERENCES

Andrulis, E. D., Guzman, E., Doring, P., Werner, J. and Lis, J. T. (2000). High-resolution localization of Drosophila Spt5 and Spt6 at heat shock genes in vivo: roles in promoter proximal pausing and transcription elongation. *Genes Dev.* **14**, 2635-2649.

Bortvin, A. and Winston, F. (1996). Evidence that Spt6p controls chromatin structure by a direct interaction with histones. *Science* **272**, 1473-1476.

Chen, J.-N. and Fishman, M. C. (1996). Zebrafish *tinman* homolog demarcates the heart field and initiates myocardial differentiation. *Development* **122**, 3809-3816.

Conaway, J. W., Shilatifard, A., Dvir, A. and Conaway, R. C. (2000). Control of elongation by RNA polymerase II. *Trends Biochem. Sci.* **25**, 375-380.

Driever, W., Solnica-Krezel, L., Schier, A. F., Neuhauss, S. C., Malicki, J., Stemple, D. L., Stainier, D. Y. R., Zwartkruis, F., Abdelilah, S., Rangini, Z. et al. (1996). A genetic screen for mutations affecting embryogenesis in zebrafish. *Development* **123**, 37-46.

Fornzler, D., Her, H., Knapik, E. W., Clark, M., Lehrach, H., Postlethwait, J. H., Zon, L. I. and Beier, D. R. (1998). Gene mapping in zebrafish using single-strand conformation polymorphism analysis. *Genomics* **51**, 216-222.

Garber, M. E. and Jones, K. A. (1999). HIV-1 Tat: coping with negative elongation factors. *Curr. Opin. Immunol.* **11**, 460-465.

Guo, S., Wilson, S. W., Cooke, S., Chitnis, A. B., Driever, W. and Rosenthal, A. (1999). Mutations in the zebrafish unmask shared regulatory pathways controlling the development of catecholaminergic neurons. *Dev. Biol.* **208**, 473-487.

Guo, S., Yamaguchi, Y., Schilbach, S., Wada, T., Lee, J., Goddard, A., French, D., Handa, H. and Rosenthal, A. (2000). A regulator of transcriptional elongation controls vertebrate neuronal development. *Nature* **408**, 366-369.

Halloran, M. C., Sato-Maeda, M., Warren, J. T., Su, F., Lele, Z., Krone, P. H., Kuwada, J. Y. and Shoji, W. (2000). Laser-induced gene expression in specific cells of transgenic zebrafish. *Development* **127**, 1953-1960.

Hartzog, G. A., Wada, T., Handa, H. and Winston, F. (1998). Evidence that Spt4, Spt5, and Spt6 control transcription elongation by RNA polymerase II in *Saccharomyces cerevisiae*. *Genes Dev.* **12**, 357-369.

Hubbard, E. J., Dong, Q. and Greenwald, I. (1996). Evidence for physical and functional association between EMB-5 and LIN-12 in Caenorhabditis elegans. *Science* **273**, 112-115.

Ivanov, D., Kwak, Y. T., Guo, J. and Gaynor, R. B. (2000). Domains in the SPT5 protein that modulate its transcriptional regulatory properties. *Mol. Cell. Biol.* **20**, 2970-2983.

Kane, D. A., Hammerschmidt, M., Mullins, M. C., Maischein, H. M., Brand, M., van Eeden, F. J., Furutani-Seiki, M., Granato, M., Haffter, P., Heisenberg, C. P. et al. (1996). The zebrafish epiboly mutants. *Development* **123**, 47-55.

Kaplan, C. D., Morris, J. R., Wu, C. and Winston, F. (2000). Spt5 and Spt6 are associated with active transcription and have characteristics of general elongation factors in *D. melanogaster*. *Genes Dev.* **14**, 2623-2634.

Lele, Z., Engel, S. and Krone, P. H. (1997). *hsp47* and *hsp70* gene expression is differentially regulated in a stress- and tissue-specific manner in zebrafish embryos. *Dev. Genet.* **21**, 123-133.

Lis, J. (1998). Promoter-associated pausing in promoter architecture and postinitiation transcriptional regulation. *Cold Spring Harb. Symp. Quant. Biol.* **63**, 347-356.

Malicki, J., Schier, A. F., Solnica-Krezel, L., Stemple, D. L., Neuhauss, S. C., Stainier, D. Y., Abdelilah, S., Rangini, Z., Zwartkruis, F. and Driever, W. (1996). Mutations affecting development of the zebrafish ear. *Development* **123**, 275-283.

Muller, F., Lakatos, L., Dantonel, J., Strahle, U. and Tora, L. (2001). TBP is not universally required for zygotic RNA polymerase II transcription in zebrafish. *Curr. Biol.* **11**, 282-287.

Nasevicius, A. and Ekker, S. C. (2000). Effective targeted gene 'knockdown' in zebrafish. *Nat. Genet.* **26**, 216-220.

Padgett, R. A., Grabowski, P. J., Konarska, M. M., Seiler, S. and Sharp, P. A. (1986). Splicing of messenger RNA precursors. *Annu. Rev. Biochem.* **55**, 1119-1150.

Rasmussen, E. B. and Lis, J. T. (1993). In vivo transcriptional pausing and cap formation on three Drosophila heat shock genes. *Proc. Natl. Acad. Sci. USA* **90**, 7923-7927.

Reiter, J. F., Alexander, J., Rodaway, A., Yelon, D., Patient, R., Holder, N. and Stainier, D. Y. R. (1999). Gata5 is required for the development of the heart and endoderm in zebrafish. *Genes Dev.* **13**, 2983-2995.

Rougvie, A. E. and Lis, J. T. (1988). The RNA polymerase II molecule at the 5′ end of the uninduced *hsp70* gene of *D. melanogaster* is transcriptionally engaged. *Cell* **54**, 795-804.

Serbedzija, G. N., Chen, J. N. and Fishman, M. C. (1998). Regulation in the heart field of zebrafish. *Development* **125**, 1095-1101.

Shimoda, N., Knapik, E. W., Ziniti, J., Sim, C., Yamada, E., Kaplan, S., Jackson, D., de Sauvage, F., Jacob, H. and Fishman, M. C. (1999). Zebrafish genetic map with 2000 microsatellite markers. *Genomics* **58**, 219-232.

Stainier, D. Y. R., Fouquet, B., Chen, J. N., Warren, K. S., Weinstein, B. M., Meiler, S. E., Mohideen, M. A., Neuhauss, S. C., Solnica-Krezel, L., Schier, A. F. et al. (1996). Mutations affecting the formation and function of the cardiovascular system in the zebrafish embryo. *Development* **123**, 285-292.

Summerton, J. and Weller, D. (1997). Morpholino antisense oligomers: design, preparation, and properties. *Antisense Nucleic Acid Drug Dev.* **7**, 187-195.

Swanson, M. S. and Winston, F. (1992). SPT4, SPT5 and SPT6 interactions: effects on transcription and viability in Saccharomyces cerevisiae. *Genetics* **132**, 325-336.

Talbot, W. S. and Schier, A. F. (1999). Positional cloning of mutated zebrafish genes. *Methods Cell Biol.* **60**, 259-286.

Wada, T., Takagi, T., Yamaguchi, Y., Ferdous, A., Imai, T., Hirose, S., Sugimoto, S., Yano, K., Hartzog, G. A., Winston, F., Buratowski, S. and Handa, H. (1998). DSIF, a novel transcription elongation factor that regulates RNA polymerase II processivity, is composed of human Spt4 and Spt5 homologs. *Genes Dev.* **12**, 343-356.

Westerfield, M. (1995). *The Zebrafish Book.* Eugene, OR: University of Oregon Press.

Winston, F. (2001). Control of eukaryotic transcription elongation. *Genome Biol.* **2**, 1006.1-1006.3.

Winston, F., Chaleff, D. T., Valent, B. and Fink, G. R. (1984). Mutations affecting Ty-mediated expression of the *HIS4* gene of *Saccharomyces cerevisiae*. *Genetics* **107**, 179-197.

Wu-Baer, F., Lane, W. S. and Gaynor, R. B. (1998). Role of the human homolog of the yeast transcription factor SPT5 in HIV- 1 Tat-activation. *J. Mol. Biol.* **277**, 179-197.

Yamaguchi, Y., Wada, T., Watanabe, D., Takagi, T., Hasegawa, J. and Handa, H. (1999). Structure and function of the human transcription elongation factor DSIF. *J. Biol. Chem.* **274**, 8085-8092.

Yamaguchi, Y., Narita, T., Inukai, N., Wada, T. and Handa, H. (2001). SPT genes: key players in the regulation of transcription, chromatin structure and other cellular processes. *J. Biochem.* **129**, 185-191.

Yelon, D., Horne, S. A. and Stainier, D. Y. (1999). Restricted expression of cardiac myosin genes reveals regulated aspects of heart tube assembly in zebrafish. *Dev. Biol.* **214**, 23-37.

Yelon, D., Ticho, B., Halpern, M. E., Ruvinsky, I., Ho, R. K., Silver, L. M. and Stainier, D. Y. R. (2000). The bHLH transcription factor Hand2 plays parallel roles in zebrafish heart and pectoral fin development. *Development* **127**, 2573-2582.

Zorio, D. A. and Bentley, D. L. (2001). Transcription elongation: the 'Foggy' is lifting. *Curr. Biol.* **11**, R144-R146.